Int. J. Electrochem. Sci., 6 **(2011)** 778 - 792

International Journal of
ELECTROCHEMICAL
SCIENCE
www.electrochemsci.org

Hydrodynamic Effects on the CO_2 Corrosion Inhibition of X-120 Pipeline Steel by Carboxyethyl-imidazoline

D.M. Ortega-Toledo[1], J.G. Gonzalez-Rodriguez[2], M.Casales[3,], A.Caceres[4] and L. Martinez[3,5]*

[1] Centro de Investigacion en Materiales Avanzados, Miguel de Cervantes 120, Chih. Mexico
[2] U.A.E.M.-C.I.I.C.Ap, Av. Universidad 1001, 6225-Cuernavaca, Mor., Mexico
[3] Universidad Nacional Autonoma de Mexico, Instituto de Ciencias Fisicas, Av. Universidad S/N, 6225-Cuernavaca, Mor., Mexico
[4]Departamento de Ingenieria Quimica Metalurgica, Facultad de Quimica, Universidad Nacional Autonoma de Mexico, 04510, Mexico, D.F., Mexico
[5] Corrosión y Proteccion Ingenieria SC, Rio Nazas 6, Cuernavaca, Morelos, Mexico. CP62290
[*]E-mail: mcasales@fis.unam.mx

Received: 23 September 2010 / *Accepted:* 1 November 2010 / *Published:* 1 March 2011

The effect of flow conditions on the performance of carboxyethylimidazoline as CO_2-corrosion inhibitor for API X-120 pipeline steel has been evaluated by using electrochemical techniques. Techniques includes polarization curves, linear polarization resistance, electrochemical impedance spectroscopy and electrochemical noise measurements, whereas the rotation speed were 0, 250, 500, 1000 and 2500 rpm. Different techniques show that for uninhibited solution, the corrosion rate increases with an increase in the rotating speed, but for the inhibited solution, the lowest corrosion rate is obtained at 1000 rpm, but it increases with a further increase in the rotating speed. Electrochemical noise measurements shows that in absence of inhibitor, the steel is susceptible to uniform corrosion, whereas when the inhibitor is present, the steel is highly susceptible to localized type of corrosion.

Keywords: Carbon steel, acid corrosion, electrochemical noise, rotating speed

1. INTRODUCTION

It is very well known that CO_2 corrosion would cause the failure of pipelines and structural components in petroleum production, resulting in significant economic losses and catastrophic accidents as well as water resource and environment pollution [1-5]. The CO_2 corrosion is complex, with a number of factors affecting the steel corrosion process [5-10]. Particularly, the fluid hydrodynamics plays a significant role through a complex interrelationship of near-wall hydrodynamic

momentum and mass transfer as well as fluid parameters defining general flow properties with the corrosion reactions of steel [11-16]. So far, corrosion inhibitor injection, especially nitrogen-based organic surfactant, such as amine, imidazoline and their salts is still the most cost-effective method to solve this problem. However, most inhibitor evaluations are generally only based on test results under stagnant conditions. There exist a limited number of studies on the effect of flow velocity on inhibitors performance. For instance, Jiang et al. [17] has carried out a study of the inhibition of CO_2 corrosion of N80 steel by quaternary alkynoxymethyl amine and imidazoline in 3% NaCl under static and flowing conditions by using a modified rotating disk apparatus. The effect of flow velocity, inhibitor concentration has been studied by using polarization curves, weight loss tests and electrochemical impedance spectroscopy (EIS) measurements. They have found an optimum inhibitor concentration under static conditions, finding a critical effect of the flow velocity depending upon inhibitor concentration. Bommersbach et al. [18] studied the inhibitor efficiency of a carboxylic acid and a tertiary amine on the corrosion of SAE 1038 carbon steel in a mixture of Na_2SO_4+Na_2CO_3+NaCl at different rotation speeds (0, 1600 and 3200 rpm) by using EIS measurements. They found that inhibitor film formation depends on electrode rotation rate: film forms faster under high rotation speeds. Ochoa et al. [19,20] studied the mechanism of inhibition of a carbon steel by a non-toxic multi-component inhibitor (fatty amines associated with phosphono-carboxylic acid salts) by using EIS measurements, and found the properties of the protective layers formed on the metal surface are dependent on the electrode rotation rate. In another work [21] Musa studied the change of open circuit potential (OCP) with immersion time, Tafel polarization, and electrochemical impedance spectroscopy (EIS) to investigate the corrosion inhibitor layer forming on mild steel surface. 4-Amino-5-phenyl-4H-1, 2, 4-trizole-3-thiol (APTT) was used through out the experiments as the corrosion inhibitor in the study. The investigation was conducted under hydrodynamic conditions with different pickling solutions of 0.5M HCl and 2.5M H2SO4 at 30 °C. The hydrodynamic conditions experiments were simulated using the rotating cylinder electrode (RCE). In both solutions, the values of OCP were shifted to more positive direction, the corrosion current densities were decreased, and charge transfer resistances were increased with flow velocity, respectively.

Among the different electrochemical techniques that can be used to evaluate inhibitors, electrochemical impedance spectroscopy (EIS) is a powerful tool in addition to traditional techniques such as polarization curves or linear polarization resistance (LPR) measurements. However, electrochemical noise (EN) measurements have also been successfully applied to the study of corrosion inhibitors performance [22-25]. These measurements are made without any external perturbation of the systems, and provide information about the actual system being studied with little possible artifacts. EN technique involves the estimation of the electrochemical noise resistance, R_n, which is calculated as the standard deviation of potential, σ_v, divided by the standard deviation of current, σ_i,

$$R_n = \sigma_v/\sigma_i \qquad [1]$$

where R_n can be taken as the linear polarization resistance, R_p in the Stern-Geary equation:

$$I_{corr} = \frac{b_a b_c}{2.3(b_a + b_c)} \frac{1}{R_P} \quad [2]$$

thus, inversely proportional to the corrosion rate, I_{corr}, but with the necessary condition that a trend removal applied over an average baseline, as previously established [26]. It has been demonstrated that the noise signal provides information about the dynamics that occur on the surface of the electrode and about the type of corrosion that is occurring, either uniform or localized. The aim of this work is to study the performance of a simple organic compound, carboxyethylimidazoline, as CO_2 corrosion inhibitor of API X-120 pipeline steel by using different electrochemical techniques such as polarization curves, LPR, EIS and EN measurements under hydrodynamic conditions.

2. EXPERIMENTAL PROCEDURE

2.1. Testing material

Material tested was an API X-120 pipeline steel with a chemical composition as given in Table 1. Cylindrical specimens 10 mm long with a diameter of 6 mm were machined and embedded in PTFE delimiting the working surface of 0.28 cm^2. This system was machined to form the rotating disk electrode, which was polished up to 2400 grade by emery-paper, rinsed with distilled water, acetone, and dried under an air flow.

Table 1. Chemical composition of X-120 steel (wt.%).

C	Si	Mn	P	S	Cr	Mo	Ni	Al	Co
0.027	0.24	1.00	0.003	0.004	0.42	0.18	1.35	0.045	0.004
Cu	Nb	Ti	Fe						
0.010	0.024	0.015	96.6						

2.2. Testing solution

Inhibitor used in this work was a commercial carboxyethylimidazoline with a general structure as shown in Fig. 1, which is composed of a five member ring containing nitrogen elements, a C-14 saturated hydrophobic head group and a pendant, hydrophilic carboxyamido group attached to one of the nitrogen atoms. Inhibitor was dissolved in pure 2-propanol.

The concentration of the inhibitor was the recommended by the manufacturer, 20 ppm at a testing temperature of 50 °C, which was kept constant with a hot plate. Testing solution consists of 3% NaCl solution, heated, de-aerated by purging with CO_2 gas during 2 hours prior the experiment and kept bubbling throughout the experiment. Inhibitor is added 2 hours after pre-corroding the specimens in the CO_2-containing solution, starting the measurements one hour later. Rotation speeds were 0. 250. 500, 1000 and 2500 rpm.

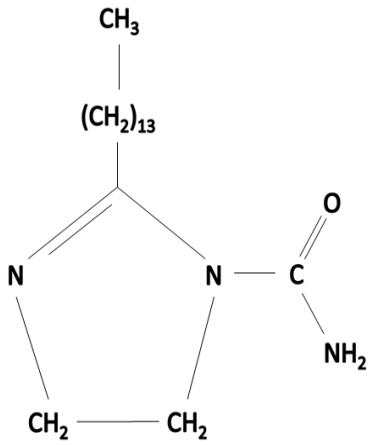

Figure 1. General structure of carboxyethylimidazoline.

2.3. *Electrochemical measurements*

Employed electrochemical techniques includes potentiodynamic polarization curves, linear polarization resistance, LPR, electrochemical impedance spectroscopy, EIS, and electrochemical noise, EN, measurements, both in current and voltage. Polarization curves were recorded at a constant sweep rate of 1 mV/s from -300 to +300 mV_{SCE} interval with respect to the open circuit potential (E_{corr}). The measurements were obtained by using a conventional three electrode glass cell with two graphite rods as auxiliary electrodes, and a saturated calomel electrode (SCE) reference electrode with a Lugging capillary bridge. Corrosion current density values, I_{corr}, were calculated by using the Tafel extrapolation method by taking an extrapolation interval of ± 250 mV_{SCE} with respect the E_{corr} value once stable. The inhibitor efficiency, η, is calculated as follows :

$$\eta\ (\%) = (I_{corr} - I'_{corr})/\ I_{corr}\ \text{X}\ 100 \qquad [3]$$

where I'_{corr} and I_{corr} are the corrosion current values with and without inhibitor, respectively. LPR measurements were carried out by polarizing the specimen ±10 mV_{SCE} with respect to E_{corr}, at a scanning rate of 1 mV/s every 20 minutes, during 24 hours. EIS tests were carried out at the E_{corr} value by using a signal with an amplitude of 10 mV_{SCE} and a frequency interval of 0.1 Hz-30 kHz. An ACM potentiostat controlled by a desk top computer was used for the LPR tests and polarization curves, whereas for the EIS measurements a PC4 300 Gamry potentiostat was used. EN measurements in both current and potential were recorded using a platinum rod as second working electrodes, 0.25 mm diameter, embedded in epoxy resin, with an effective exposed area of 4.9 mm^2, and a reference SCE electrode. EN measurements were made recording simultaneously the potential and current fluctuations at a sampling rate of 1 point per second. A fully automated zero resistance ammeter (ZRA) from ACM instruments was used in this case. Finally, the noise resistance, $R_{n,}$ was then calculated as the ratio of the potential noise standard deviation, $\sigma_{v,}$ over the current noise standard deviation, σ_{i}, according to Eq. [1].

3. RESULTS AND DISCUSSION

Polarization curves for X-120 steel in uninhibited CO_2-saturated 3% NaCl solution in stagnant and stirred solutions are shown in Fig. 2. This figure shows only an active behavior in the anodic branch of the curve, with the current increasing with the applied potential without the presence of a passive layer. The anodic current density value remains more or less constant regardless of the rotating speed. Dislike this, the cathodic current density exhibited a limiting value, which increases as the rotating speed increases, which is due to the fact that more oxygen is transported towards the steel surface as the rotating speed increases.

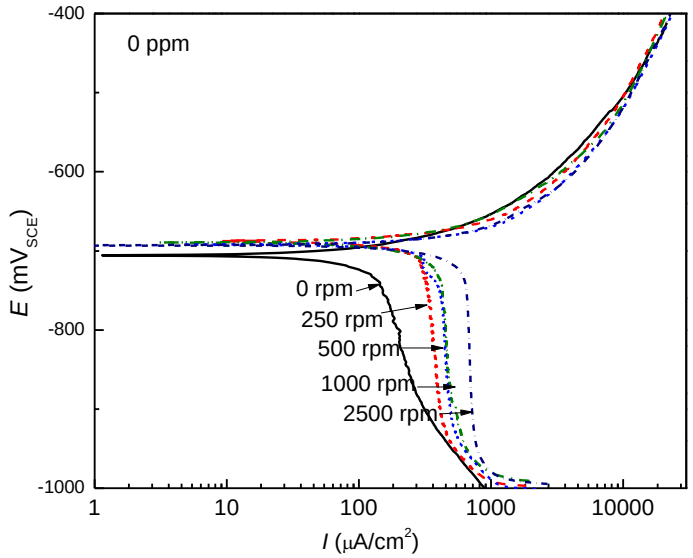

Figure 2. Effect of rotation speed in the polarization curve for X-120 steel in uninhibited CO_2-saturated 3% NaCl solution.

The free corrosion potential value, E_{corr}, becomes nobler as the rotating speed increases and the corrosion current density value, I_{corr}, increases with the rotating speed.

Table 2. Electrochemical parameters obtained from polarization curves.

Carboxyethylimidazoline concentration (ppm)		0 rpm	250 rpm	500rpm	1000 rpm	2500 rpm
0	E_{corr} (mV_{SCE})	-710	-695	-690	-690	-690
	I_{corr} ($\mu A/cm^2$)	140	280	380	420	630
80	E_{corr} (mV_{SCE})	-640	-605	-624	-610	-615
	I_{corr} ($\mu A/cm^2$)	38	20	170	270	170

Table 2 summarizes these results. A similar behavior is observed for the solution containing 20 ppm of carboxyethylimidazoline, Fig. 3: the limit cathodic current density value increases with the

rotating speed, reaching its highest value by stirring the solution at 1000 rpm, and it decreases with a further increase in the rotation speed of 2500 rpm. However, at potential values nobler than -520 mV_{SCE} an anodic limit current density is observed at all rotating speed values, which could be to the diffusion of electrolyte through a film formed inhibitor. In all cases, the I_{corr} values for the inhibited solution are lower than those obtained for the uninhibited solution at the same rotating speed. It is generally accepted that the first step during the adsorption of an organic inhibitor on a metal surface usually involves replacement of water molecules absorbed on the metal surface:

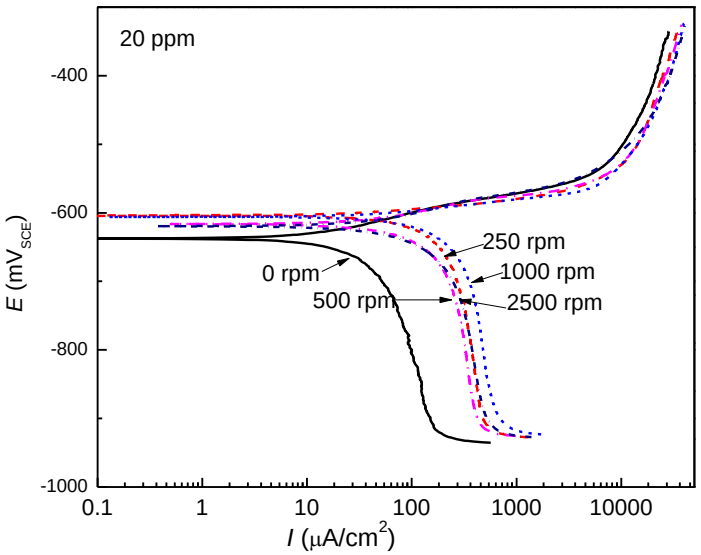

Figure 3. Effect of rotation speed in the polarization curve for X-120 steel in CO_2-saturated 3% NaCl solution containing 20 ppm of carboxyethylimidazoline.

$$Inh_{sol} + xH_2O_{ads} \rightarrow Inh_{ads} + xH_2O_{sol} \quad [4]$$

The inhibitor may then combine with freshly generated Fe^{2+} ions on steel surface, forming metal inhibitor complexes [27, 28]:

$$Fe \rightarrow Fe^{2+} + 2e \quad [5]$$

$$Fe^{2+} + Inh_{ads} \rightarrow [Fe\text{-}Inh]_{ads}^{2+} \quad [6]$$

The resulting complex, depending on its relative solubility, can either inhibit or catalyze further metal dissolution. At low concentrations the amount of carboxyethylimidazoline is insufficient to form a compact complex with the metal ions, so that the resulting adsorbed intermediate will be readily soluble in the acidic environment. But at relatively higher concentrations more carboxyethylimidazoline molecules become available for complex formation, which subsequently

diminishes the solubility of the surface layer, leading to improve the inhibition of metal corrosion, because under flow conditions there are several different effects on inhibition performance:

1. Flow can increase mass transport of inhibitor molecules that causes more inhibitor presence at metal surface. This effect can improve the inhibitor performance [29];
2. Hydrodynamic conditions can increase mass transport of metal ions (Fe^{2+}) produced during metal dissolution from electrode surface to the bulk of solution and hence lead to less $[Fe\text{-}Inh]^{2+}$ complex presence on electrode; this is a harmful effect for inhibition performance;
3. The high shear stress resulted from high flow velocity can also separate inhibitor layer of adsorbed $[Fe\text{-}Inh]^{2+}$ complex and cause more desorption from metal surface, which acts as a negative factor on inhibitor efficiency [29]. The balance of the above mentioned effects lead to changes on inhibitor efficiency with rotation rate.

The above obtained results are confirmed by the change in the polarization resistance value with time, R_p, at the different rotation speeds as shown in Fig. 4.

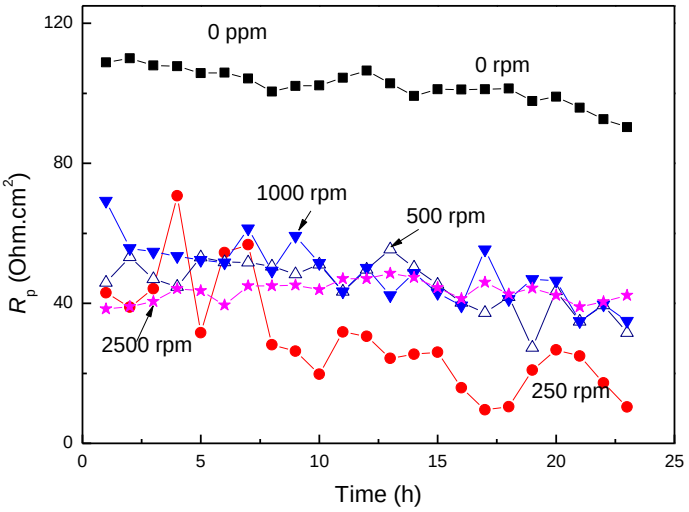

Figure 4. Effect of rotation speed in the change of the R_p value with time for X-120 steel in uninhibited CO_2-saturated 3% NaCl solution.

This figure shows that the highest R_p value, thus the lowest corrosion rate, is obtained under stagnant conditions, and this value decreases as the rotation speed increases which is due to an increase in the mass transfer of dissolved oxygen from electrolyte to the interface. On the other hand, for inhibited solution, Fig. 5, for rotating speeds lower than 1000 rpm, an increase in the rotating speed decreases the R_p value, as compared to that value in stagnant conditions, but it reaches a maximum value at 1000 rpm; a further increase in the rotating speed brings a decrease in the R_p value, increasing, thus, the corrosion rate.

Nyquist and Bode plots for uninhibited solution at the different rotating speeds are shown on Fig. 6. Nyquist plot shows a capacitive semicircle at high and intermediate frequency values, Fig. 6a, which arise from the charge transfer from the metal to electrolyte through the double electrochemical layer. The diameter of this semicircle, the charge transfer resistance, R_{ct}, is equivalent to the polarization resistance, R_p, and it decreases as the rotating speed increases, increasing, thus, the corrosion rate, as shown by polarization curves, Fig. 2, and the R_p values, Fig. 4. At lower frequencies, a small inductive loop can be observed at all rotating speeds, which is due to relaxation process obtained by the adsorption of species such as $[H^+]_{ads}$ on the electrode surface.

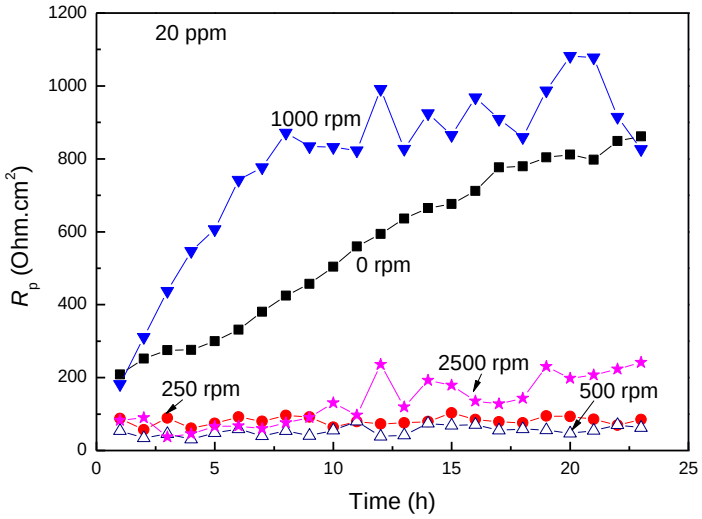

Figure 5. Effect of rotation speed in the change of the R_p value with time for X-120 steel in CO_2-saturated 3% NaCl solution containing 80 μmol/l of carboxyethylimidazoline.

This loop does not disappear as the rotating speed increase, indicating that the adsorbed species remain on the steel surface. On the other hand, Bode plots show only a peak around 50 Hz, Fig. 6 b, and remains constant with increasing the rotating speed. No evidence of any protective layer was found due to the presence of only one peak.

For inhibited solution, Nyquist diagrams show a capacitive semicircle at all rotating speed values except at 10000 rpm, Fig. 7a, where two semicircles are observed: one at high and intermediate frequency values, which is due to the charge transfer from metal to electrolytethrough the double electrochemical layer, and a second semicircle at lower frequencies, due to the presence of a film formed by the inhibitor. The highest semicircle diameter value, and thus the lowest corrosion rate, is obtained with a rotation speed of 1000 rpm, a further increase in the rotation speed of 2500 rpm brings a decrease in the semicircle diameter. Bode diagrams, Fig. 7 b, shows a peak at 500 and 2500 rpm but two peaks at 0, 250 and 1000 rpm, indicating the presence of a film formed by the inhibitor at these rotation speeds.

To study the susceptibility of this steel towards a localized type of corrosion, some electrochemical noise tests in both potential and current were performed, and Fig. 8 shows some

typical time series for the noise in potential at different rotating speeds for uninhibited solution. Time series at 0 rpm consist of transients with low intensity and high frequency, combined with some transients of higher intensity but lower frequency, indicating a mixture of uniform and localized type of corrosion. As the rotating speed increases, both the intensity and frequency of the transients increases, indicating that the steel surface is now susceptible towards a uniform type of corrosion. This is consistent with the fact that as the rotating speed increases the amount of dissolved oxygen that reaches the steel surface increases, increasing, thus, the corrosion rate as shown by Figs. 2 and 4. When inhibitor is added, Fig. 9, the time series under stagnant conditions consists of transients of low intensity and low frequency, but both the intensity and frequency increases with an increase in the rotation speed.

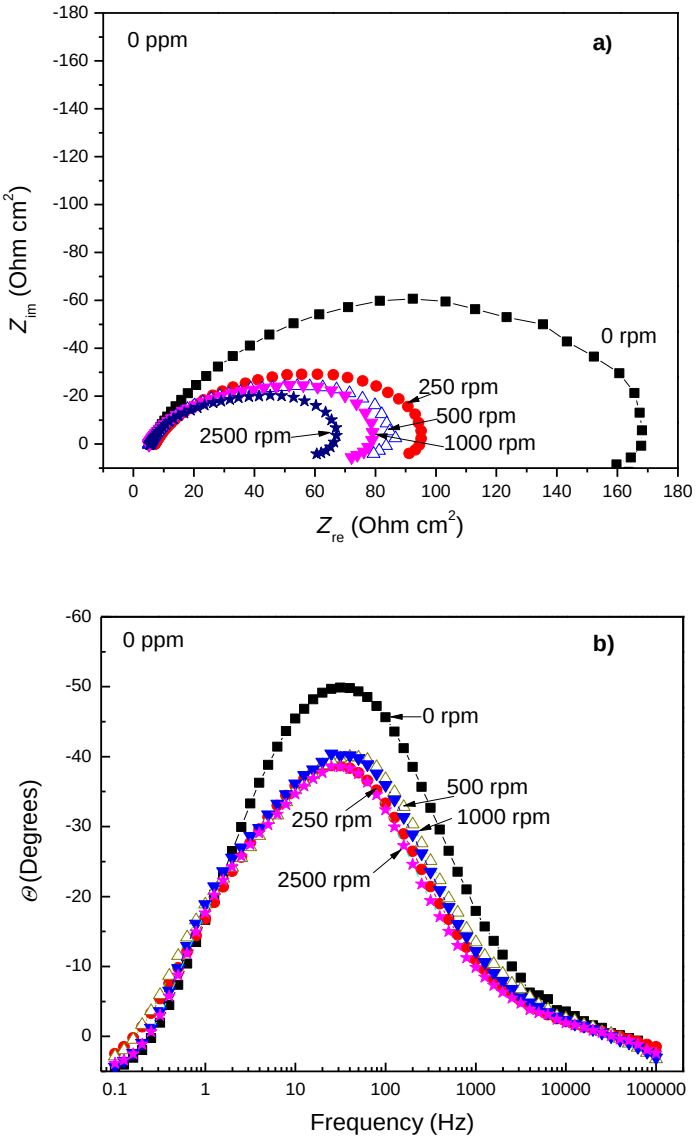

Figure 6. Effect of rotation speed in the EIS data for X-120 steel in uninhibited CO_2-saturated 3% NaCl solution in the a) Nyquist and b) Bode format.

These transients are due to the breakdown of any film formed on the steel surface and they are typical of a localized type of corrosion pitting-like [30]. This is because although the inhibitor in transported to the electrode surface as the rotating speed increases, some places remain uncovered by the inhibitor, and these places remain as active sites where a localized type of corrosion takes place.

The combined effect of potential standard deviation, σ_V, and current standard deviation, σ_I, results in the noise resistance value, R_n, (eq. [1]) which is inversely proportional to the corrosion rate, I_{corr}, as previously done with the R_p values, Fig. 4. An estimation of the corrosion rate can be completed through the variation of R_n with time for the different rotation speeds, as can be seen in Figs. 10 and 11 for uninhibited and inhibited solutions respectively.

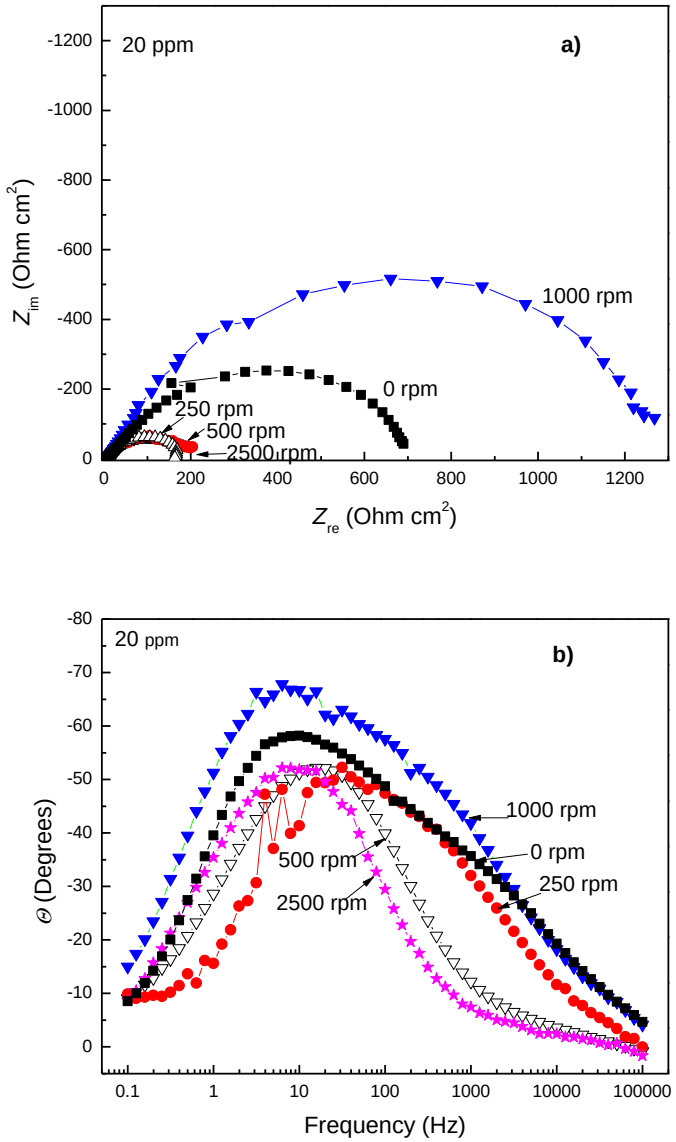

Figure 7. Effect of rotation speed in the EIS data for X-120 steel in CO_2-saturated 3% NaCl solution containing 20 ppm of carboxyethylimidazoline in the a) Nyquist and b) Bode format.

The behavior for uninhibited solution is very similar to that observed by R_p in Fig. 4 although with much more fluctuations for the R_n values, with the highest R_n value obtained under stagnant conditions and decreasing as the rotating speed increases.

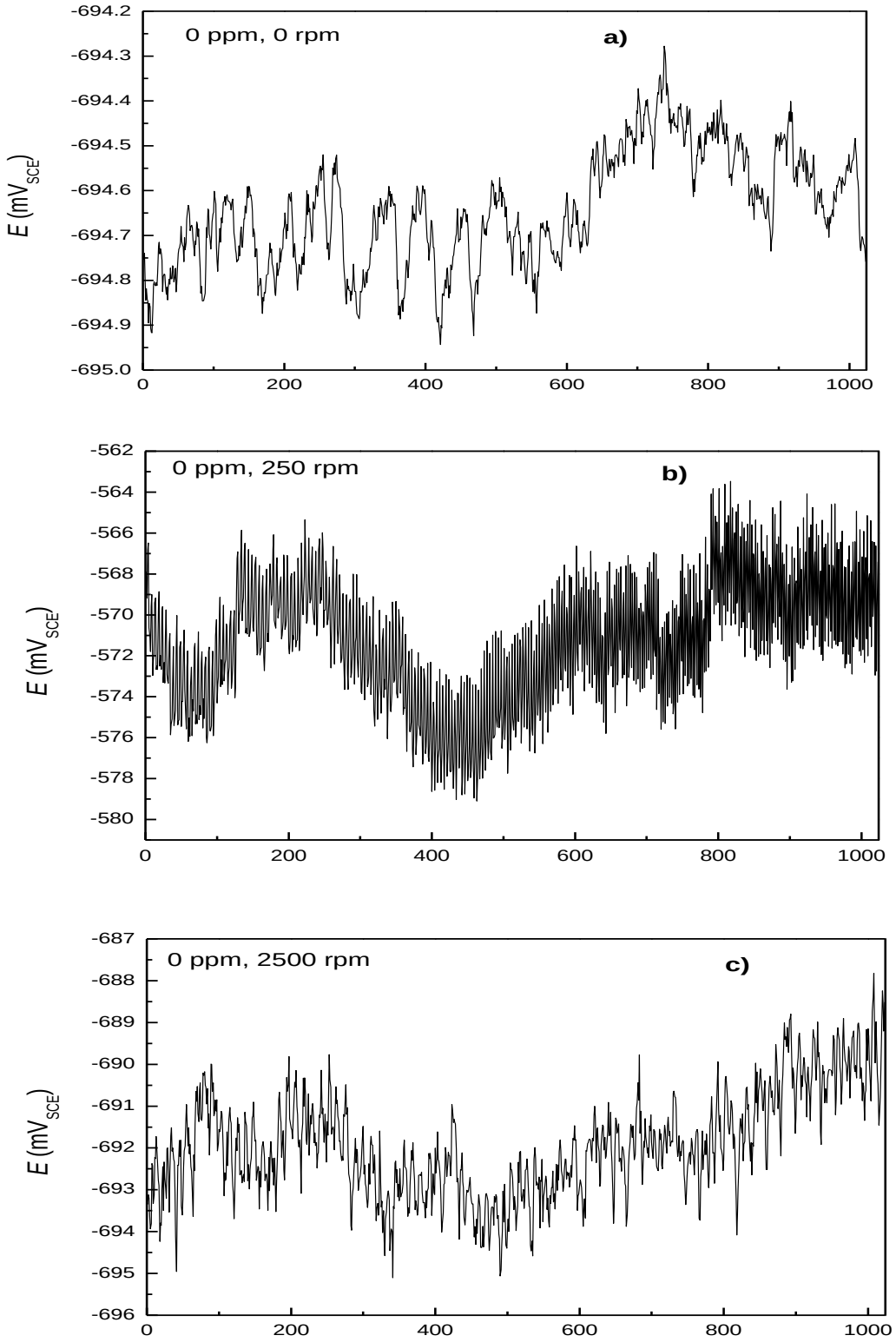

Figure 8. Noise in potential for X-120 steel in uninhibited CO_2-saturated 3% NaCl solution at a) 0, b) 250 and c) 2500 rpm.

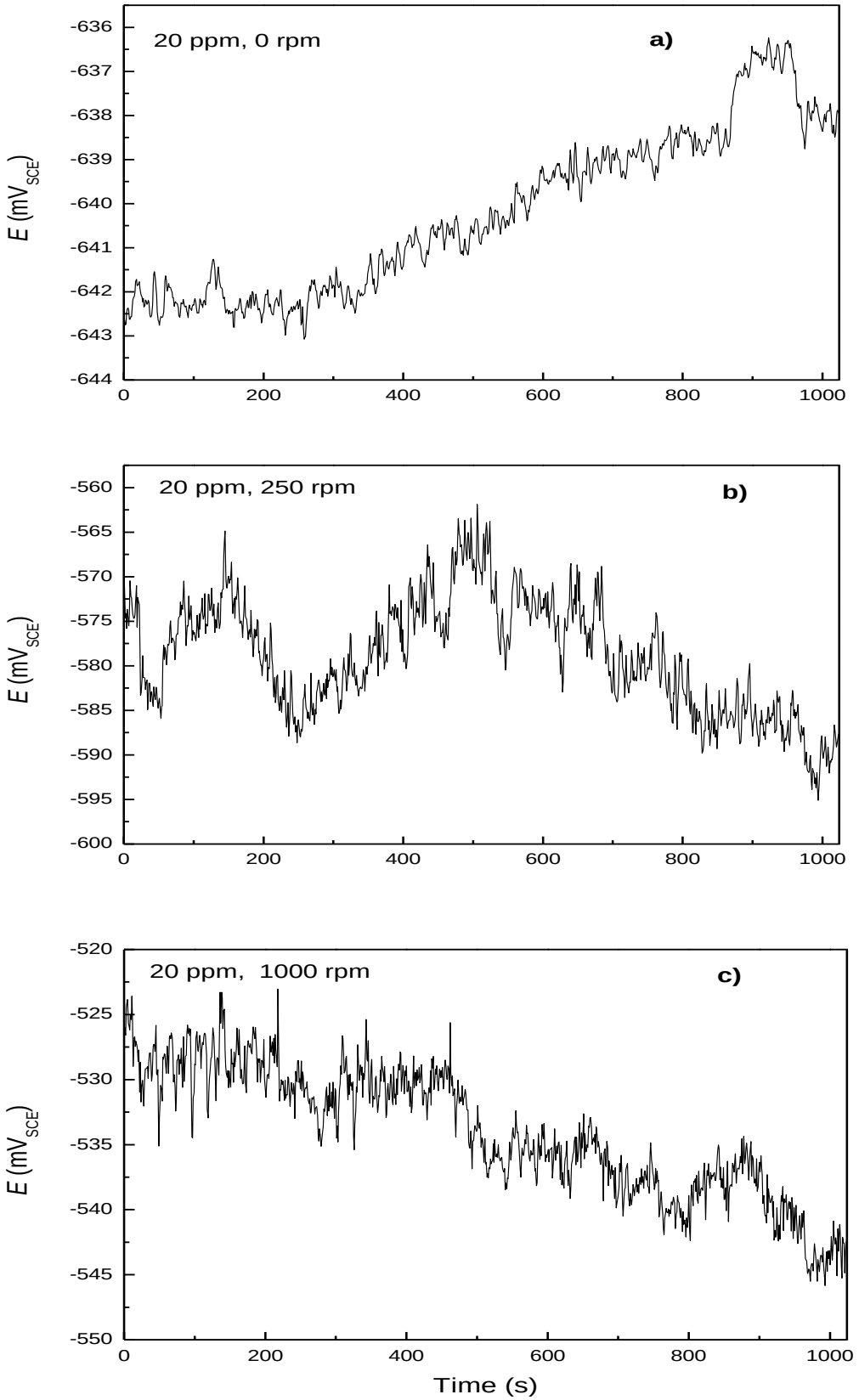

Figure 9. Noise in potential for X-120 steel in CO_2-saturated 3% NaCl solution containing 20 ppm of carboxyethylimidazoline at a) 0, b) 250 and c) 1000 rpm.

Thus, for uninhibited solution, noise data indicate that the lowest corrosion rate is obtained in static conditions. For inhibited solution, Fig. 11 shows that the highest R_n value is obtained at a rotating speed of 1000 rpm, with a decrease in its value with a further increase in the rotation speed up to 2500 rpm, similar to the exhibited by R_p in Fig. 5.

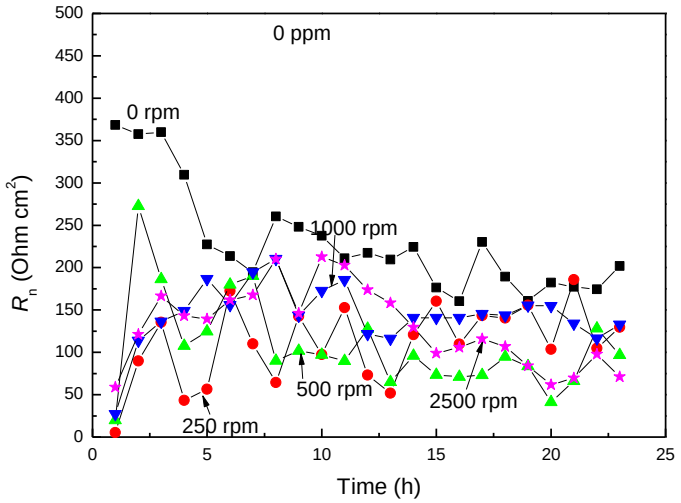

Figure 10. Effect of rotation speed in the change of R_n with time for X-120 steel in uninhibited CO_2-saturated 3% NaCl solution.

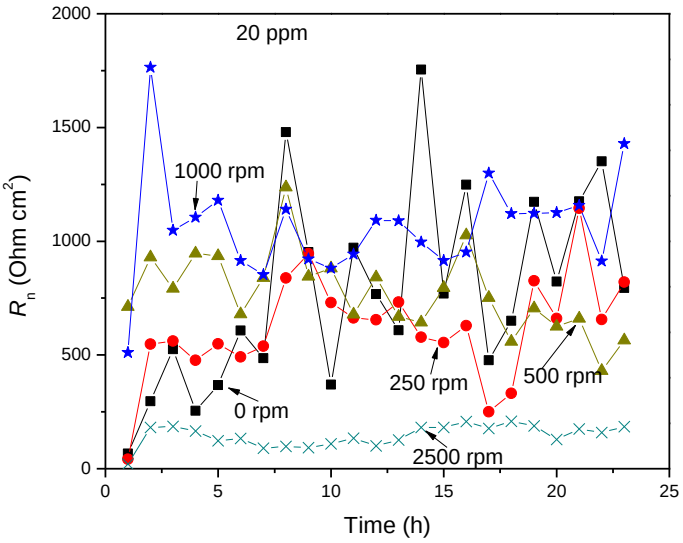

Figure 11. Effect of rotation speed in the change of R_n with time for X-120 steel in CO_2-saturated 3% NaCl solution containing 20 ppm of carboxyethylimidazoline.

4. CONCLUSIONS

A study on the effect of rotation speed on the CO_2 corrosion inhibition of X-120 pipeline steel by carboxyethylimidazoline has been carried out by using electrochemical techniques. Different

techniques have shown that for uninhibited solution, an increase in the rotating speed increased the corrosion rate, but for the inhibited solution, the corrosion rate decreased with a rotating speed of 1000 rpm, but it increased again with a further increase in the rotating speed. Additionally, EN measurements have shown that for uninhibited solution, the steel was susceptible to uniform type of corrosion, whereas for the inhibited solution, the film formed by the inhibitor leaves some active sites, making the steel susceptible to localized corrosion.

ACKNOWLEDGEMENTS
D. M. Ortega and A. Caceres acknowledge CONACYT – MEXICO for the support of a graduate scholarship to CIMAV and FQ-UNAM. Corrosion y Proteccion Ingeniería SC and ICF-UNAM acknowledge the support of grant FOMIX MOR-2008-C01-93689.

References

1. D.A. Lopez, S.N. Simison, S.R. de Sanchez, *Electrochim. Acta* 48 (2003) 845.
2. M.B. Kermani, A. Morshed, *Corros.* 59 (2003) 659.
3. B.R. Linter, G.T. Burstein, *Corros. Sci.* 42 (1999) 117.
4. Z. Xia, K.C. Chou, Z.S. Smialowzka, *Corrosion* 45 (1989) 636.
5. S. Nesic, *Corros. Sci.* 49 (2007) 4308.
6. K. Videm, J. Kvarekval, *Corrosion* 51 (1991) 260.
7. T. Hong, Y.H. Sun, W.P. Jepson, *Corros. Sci.* 44 (2002) 101.
8. G.I. Ogundele, W.E. White, *Corrosion* 42 (1986) 71.
9. S. Nesic, J. Postlethwaite, S. Olsen, *Corrosion* 52 (1996) 280.
10. D.A. Lopez, W.H. Scheiner, S.R. de Sanchez, S.N. Simison, *Appl. Surf. Sci*. 207 (2003) 69.
11. G.T. Burstein, K.Sasaki, *Corros. Sci.* 42 (2000) 841.
12. K.D. Efird, E.J. Wright, J.A. Boros, T.G. Hailey, *Corrosion* 49 (1993) 992.
13. S. Zhou, M.M. Stack, R.C. Newman, *Corros. Sci.* 38 (1996) 1071.
14. E.A.M. Hussain, M.J. Robinson, *Corros. SCi*. 49 (2007) 1737.
15. K. Sasaki, G.T. Burstein, *Corros. Sci*. 49 (2007) 92.
16. L. Quej-Aké1, R. Cabrera-Sierra, E. Arce-Estrada and J. Marín-Cruz, *Int. J. Electrochem. Sci.,* 3 (2008) 56.
17. X. Jiang, Y.G. Zheng, W. Ke, *Corros. Sci.* 47 (2005) 2636.
18. Pascale Bommersbach, Catherine Alemany-Dumont, Jean-Pierre Millet, Bernard Normand, *Electrochim. Acta* 51,(2006) 4011.
19. Nathalie Ochoa, Francis Moran, Nadine Pébère, Bernard Tribollet, *Corros. Sci*. 47 (2005) 593.
20. Nakarin Srisuwan, Nathalie Ochoa, Nadine Pébère, Bernard Tribollet, *Corros. Sci*. 50 (2008) 1245.
21. Ahmed Y. Musa1, Abdul Amir H. Kadhum, Abu Bakar Mohamad, Abdul Razak Daud, Mohd Sobri Takriff , Siti Kartom Kamarudin, Norhamidi Muhamad, *Int. J. Electrochem. Sci*., 4 (2009) 707.
22. A.Popova, S. Raicheva, E Sokolova, M.Christov, *Langmuir* 12 (1996) 2083.
23. L. Nykos, T. Pajlossy, *Electrochim. Acta* 30 (1985)1533.
24. E. Garcia-Ochoa, J. Genesca, *J. Surf. and Coat. Technol.* 184 (2004) 322.
25. E. Samiento-Bustos, J.G. González Rodriguez, J. Uruchurtu, G. Dominguez-Patiño, V.M. Salinas-Bravo, *Corros. Sci*. 50 (2008) 2296.
26. P.H. Tewart, A.B. Campbell, Can, J, *Chem*, 57 (1979) 188.
27. E.E. Oguzie, Y. Li, F.H. Wang, *J. Colloid Interface Sci.* 310 (2007) 90.
28. V. Branzoi, F. Branzoi, M. M. Baibarac, *Mater. Chem. Phys*. 65 (2000) 288.

29. X. Jiang, Y.F. Zheng, W. Ke, *Corros. Sci.* 47 (2005) 2636.
30. K. Hladky, J.L. Dawson, *Corros. Sci*. 22 (1982) 23.

© 2011 by ESG (www.electrochemsci.org)